Influence of gain and index guiding on the mode structure and performance of a Raman amplifier

K. S. Repasky, J. K. Brasseur, J. G. Wessel, and J. L. Carlsten
Physics Department, Montana State University, Bozeman, Montana 59717
(Received 23 July 1996; revised manuscript received 19 February 1997)

The amplified Stokes beam's mode structure in the Raman amplifier, which comes from the interplay of gain guiding and index guiding, is studied both numerically and experimentally in this paper. Theoretical results predict that gain and index guiding will lead to a narrower amplified Stokes beam of higher output energy when the input Stokes signal is detuned to the blue side of the Raman resonance. In addition, the results show that the coupling strength of an input Stokes beam into the Raman amplifier is related to the spatial overlap of the input Stokes mode with the mode supported by the Raman amplifier. Overall there is a competition between diffraction and the nonlinear effects of gain and index guiding. Theoretical calculations predict that the coupling of the Gaussian input signal mode into the amplifier is optimized by shifting the focus of the input signal towards the entrance to the Raman amplifier, shortening the Rayleigh range on the input signal with respect to the pump beam, and detuning the input signal to the blue side of the Raman resonance, all of which are contrary to the common usage of the Raman amplifier. A discussion of these phenomena in terms of a nonorthogonal mode description of the amplifier is given. [S1050-2947(97)02107-0]

PACS number(s): 42.60.−v

I. INTRODUCTION

Understanding the spatial structure of the amplified field in an optical amplifier is critical in understanding how to optimize the performance of an optical amplifier [1–4]. Two effects that can change the spatial structure of the amplified beam are gain guiding [5–7] and index guiding [8,9]. Both gain and index guiding can occur whenever the amplifier gain is nonuniform in the transverse direction. Nonuniform gain in an optical amplifier in the transverse direction occurs when the amplifier is pumped by a beam whose intensity varies in the transverse direction. A common example for the Raman amplifier occurs when the Raman medium is pumped by a focused Gaussian beam [10–12].

For a focused Gaussian pump beam, the center of the gain profile, which is proportional to the pump intensity, amplifies the center of the signal more than the wings because the gain is larger near the center of the Gaussian gain profile. Because the center of the signal grows more than the wings, the amplified field narrows. Thus gain guiding can narrow the amplified field in an optical amplifier.

In an amplifier with a gain due to the imaginary part of the optical susceptibility, a real part of the optical susceptibility will also exist from the Kramer-Kronig relationships [13]. This real part of the susceptibility will lead to a nonuniform transverse index of refraction that can lead to index guiding. Thus both gain and index guiding will be present in an optical amplifier with a nonuniform gain in the transverse direction.

Efficient coupling of an input signal into an optical amplifier requires that the input signal mode strongly overlap the dominant amplifier mode that has the highest growth rate. When the structure of the input signal mode, including the phase fronts, exactly matches the dominant amplifier mode, all of the input signal is available to gain at the highest growth rate. However, if the pump wavelength is different from the signal wavelength or nonlinear effects are occurring in the optical amplifier, it may not be clear how or even if the input signal mode can exactly overlap the dominant amplifier mode. If, for example, the phase fronts of the input signal mode and dominant amplifier mode are not matched, interference effects can lower the coupling between these two modes, thus diminishing the performance of the amplifier. Manipulating the structure of the input signal mode to match the dominant amplifier mode can increase the output of the amplifier by forcing the input signal mode to overlap the dominant amplifier mode [1–4].

Understanding the structure of the input signal mode and the dominant mode of the optical amplifier is crucial in understanding how to manipulate the structure of the input signal mode to better overlap the dominant amplifier mode. The structure of the dominant amplifier mode is determined by the physical parameters of the optical amplifier and is difficult to change. Changing the structure of the input signal mode is much simpler and for this reason changes in the structure of the input signal are considered in this paper.

The coupling of a Gaussian input signal mode into the dominant mode of a gain [1,2,5–7] and index [8,9] guided Raman amplifier with a focused Gaussian gain profile is considered in this paper. However, the ideas presented here can be used to enhance the performance of other gain and index guided amplifiers such as with x-ray lasers [14]. Some degree of gain and index guiding can be expected to occur whenever the amplifier gain is nonuniform in the transverse direction.

The mode structure supported by the Raman amplifier arises from a complex interplay between gain guiding, index guiding, and diffraction. Gain guiding is a nonlinear effect that causes the dominant mode supported by the Raman amplifier to be narrower than the diffraction limit and because the dominant amplifier mode is narrower, it tries to diffract faster. Index guiding is also a nonlinear effect that affects the structure of the dominant amplifier mode. Index guiding oc-

curs when the input signal is detuned from the Raman resonance, yielding a real term in the Raman susceptibility that affects the index of refraction [9,13] and causes the dominant mode to focus or defocus depending on which side of the Raman resonance the input signal is detuned to.

The photorefractive effect [15,16] has been used to modify the spatial structure of a beam propagating through a crystal. This effect can be used to compensate for the effects of diffraction and allow the beam to propagate without changing its radius. The gain and index guiding effects can also be used to compensate for diffraction in a Raman amplifier. However, no amplifier parameters have been found yet that lead to an amplified Stokes beam that propagates with the gain and index guiding, exactly compensating for diffraction.

A recent experiment [4] was performed in which the structure of the Gaussian input signal mode was modified by changing its focus and Rayleigh range relative to the dominant mode of the Raman amplifier. The output of the Raman amplifier was increased by over 70% without changing the pump laser power or input signal power. In this paper we will study in more detail the mechanisms behind this result.

A recent experiment [9] also looked at the effects of index guiding in a Raman amplifier. The index guiding results in a higher Stokes output when the input signal is detuned to the blue side of the Raman resonance. The enhanced gain due to index guiding results from focusing the dominant mode supported by the Raman amplifier to a smaller spot size so that it overlaps a more intense part of the pump beam that provides the gain mechanism and hence experiences a larger gain.

The key to understanding how the coupling of the Gaussian input signal mode into the dominant amplifier mode is enhanced by modifying the structure of the Gaussian input signal mode and detuning the input signal to the blue side of the Raman resonance lies in understanding the structure of both the input signal mode and dominant amplifier mode. This paper studies the structure of the input signal and dominant amplifier mode including the effects of gain and index guiding. The enhanced coupling is also studied in terms of the structure of the input signal and dominant amplifier mode.

This paper is organized as follows. Section II contains a brief review of the nonorthogonal modes that describe the Raman amplifier. The mode structure of the dominant mode of the Raman amplifier including both gain and index guiding is discussed in Sec. III. An experiment is described in Sec. IV that allows the measurement of the spatial structure of the amplified Stokes beam at the exit of the Raman amplifier and Sec. V contains the experimental results. In Sec. VI the effects of changing the structure of the Gaussian input signal mode and detuning the input signal to the blue side of the Raman resonance to enhance the coupling of the input signal into the dominant mode of the amplifier is studied. Section VII contains some concluding remarks.

II. THEORY

In this section the wave equation that describes the Raman amplifier and includes the total Raman susceptibility [9,11] is shown. A brief description of the solution to the wave equation that yields the nonorthogonal modes is then presented.

The growth of the amplified Stokes field traveling in the positive z direction can be described by the slowly varying Maxwell wave equation in the steady-state paraxial limit. In cgs units the amplified field obeys [7–9,17]

$$\nabla_T^2 E_s(z,r_T) - 2ik_s\partial_z E_s(z,r_T) + ik_s g(z,r_T)\left(\frac{\Gamma^2}{\Delta^2+\Gamma^2} - i\,\frac{\Gamma\Delta}{\Delta^2+\Gamma^2}\right)E_s(z,r_T) = 0, \tag{1}$$

where $\nabla_T^2 = \partial_x^2 + \partial_y^2$ is the transverse Laplacian, $E_s(z,r_T)$ is the slowly varying Stokes field, k_s is the wave vector of the Stokes field, and $g(z,r_T)\Gamma^2/(\Delta^2+\Gamma^2)$ is the gain that results from the imaginary part of the Raman susceptibility. The gain explicitly includes Γ, the Raman linewidth [18], and Δ, the detuning where $\Delta = \omega_v - (\omega_p - \omega_s)$, with ω_v the resonant frequency of the Raman active medium, ω_p the pump laser frequency, and ω_s the input signal or Stokes frequency. $g(z,r_T)\Gamma\Delta/(\Delta^2+\Gamma^2)$ is the index term, which results from the real part of the Raman susceptibility and also includes explicitly the Raman linewidth and detuning. When the detuning is set equal to zero Eq. (1) reduces to the wave equation presented in Ref. [7] with no noise term to account for spontaneous scattering. It has been shown that an input signal of only a few nanowatts is enough to dominate the quantum noise in a Raman amplifier [12]. The experiments we consider are assumed to utilize an input signal much larger than a few nanowatts, so noise effects may be neglected.

The gain profile [3,7,9] takes into account the focused nature of the pump beam and is written

$$g(z,r_T) = \frac{4G}{k_g\omega_g^2(z)}\exp[-2r^2/\omega_g^2(z)], \tag{2}$$

where G is related to the pump energy [19] and plane-wave gain coefficient [20], k_g is the wave vector of the pump laser, and $\omega_g(z) = \omega_g(0)\sqrt{1+(z/z_{0g})^2}$ is the waist of the pump laser where z_{0g} is the Rayleigh range. The solution to the wave equation is found by expanding the Stokes field over a nonorthogonal modal basis [1,2,6,7,14,21]. The Stokes field is written [7]

$$E_s(z,r_T) = \beta\sum_{l,n} a_n^l(z)\Phi_n^l(z,r_T), \tag{3}$$

where β is a constant and $a_n^l(z)$ is the amplitude of the nonorthogonal mode $\Phi_n^l(z,r_T)$. The nonorthogonal modes are constructed from a superposition of the Gauss-Laguerre modes and are written

$$\Phi_n^l(z,r_T) = \sum_p b_{n,p}^l U_p^l(z,r_T), \tag{4}$$

where $U_p^l(z,r_T)$ are the Gauss-Laguerre modes and are defined in Ref. [17].

At high gains the output of the Raman amplifier is described by the lowest-order nonorthogonal mode because its growth rate is largest [7]. Therefore, nearly all the Stokes

power will be contained in this mode. The lowest-order nonorthogonal mode $\Phi_0^0(z,r_T)$ is written

$$\Phi_0^0(z,r)=\sum_p b_{0,p}^0(z)U_p^0(z,r_T). \tag{5}$$

Because the lowest-order nonorthogonal mode is made up of a superposition of several Gauss-Laguerre modes, the curvature of the phase fronts can be very different from the phase fronts of the Gaussian input signal mode. The mode structure of the lowest-order nonorthogonal mode is studied numerically in Sec. III. The spatial structure of the lowest nonorthogonal mode that describes the amplified Stokes beam at the Raman amplifier output is studied numerically and experimentally in Secs. IV and V. The largest projection of the Gaussian input signal onto the lowest-order nonorthogonal mode occurs when the phase fronts of the lowest-order nonorthogonal mode and Gaussian input signal mode are matched. However, the wave fronts of the nonorthogonal mode are very complicated and how best to match phase fronts at the input to the Raman amplifier is a difficult question that requires detailed knowledge of the structure of the lowest-order nonorthogonal mode. This is studied in detail in Sec. VI.

III. NONORTHOGONAL MODE STRUCTURE

The phase fronts and spatial structure of the lowest-order nonorthogonal mode and Gaussian input signal mode are studied in this section for two cases. The first case occurs when the input signal is tuned exactly to the Raman resonance $\Delta=0$ and therefore the Raman susceptibility is purely imaginary, which leads to gain without any index effects. This case will allow us to understand how gain guiding affects the nonorthogonal mode. In the second case, $\Delta\neq 0$ and the Raman susceptibility contains both an imaginary term and a real term. In this case the real term in the Raman susceptibility leads to an index of refraction and gives rise to index guiding. Thus, in this second case there will be both index guiding and gain guiding.

Unless otherwise noted, the Rayleigh range was set at $\sqrt{2}$ cm for both the pump and input signal. For parameters typical of Raman scattering experiments [4,9], the differences in the phase fronts would be difficult to show in the figures. Therefore, the waist and wavelengths were chosen so that the differences between the phase fronts can be easily seen in the figures. This makes the physical explanations of the mode structure and coupling easier to understand. A gain $G=3$ and a pump beam waist $\omega_g(0)=1$ cm were used. The Raman linewidth was set at 500 MHz and the detuning used was $\Delta=0$ for the on-resonance case and $\Delta=\pm 50$ MHz for the off-resonance case. The entrance to the Raman amplifier was at $z/z_{0g}=-2$.

Figure 1 shows the phase fronts for case 1 in which $\Delta=0$. The solid line shows the phase fronts for the lowest-order nonorthogonal mode, while the dashed line shows the phase fronts of the Gaussian input signal mode. The phase fronts are plotted at various locations in the cell defined by z/z_{0g} with the Gaussian input signal mode focusing at $z/z_{0g}=0$. For $z/z_{0g}<0$ notice that the curvature of the phase fronts of the Gaussian input signal mode indicate that the input signal is focusing, while for $z/z_{0g}>0$ the curvature of the phase fronts indicate that the input signal is diffracting. This is not surprising since the input signal is a simple focused Gaussian. However, the phase fronts of the nonorthogonal mode are much more complicated and very different from the Gaussian input signal mode. The phase fronts for the nonorthogonal mode for case 1 result from a competition between gain guiding and diffraction and is discussed below. Notice that the phase fronts of the nonorthogonal mode and Gaussian input signal are very poorly matched. This indicates that the Raman amplifier is not being used efficiently.

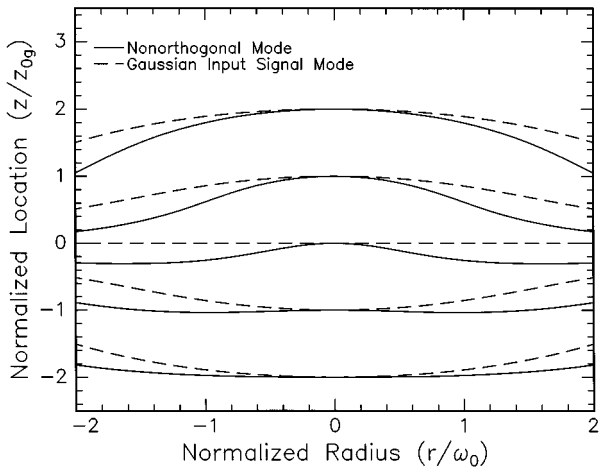

FIG. 1. Plot of the phase front of the dominant nonorthogonal mode (solid line) and Gaussian input signal mode (dashed line) at various locations in the Raman amplifier. The nonorthogonal modes are swept back from the Gaussian input mode as a result of gain guiding and diffraction. The phase overlap of the two modes is poor, indicating poor amplifier performance.

Gain guiding [5–7] has the effect of narrowing the Stokes beam as it grows in the Raman amplifier. Gain guiding works to narrow the Stokes beam because the gain that is proportional to the pump laser intensity is highest when the transverse radius $r_T\rightarrow 0$, so that the center part of the Stokes beam grows faster than the wings and hence the Stokes beam narrows. However, as the Stokes beam becomes narrower it tends to diffract faster. The competition between gain narrowing and diffraction causes the nonorthogonal mode to have phase fronts that are swept back from the input signal Gaussian mode, indicating a higher rate of diffraction for the nonorthogonal mode that is compensated by the gain narrowing.

Figure 2 shows the spatial structure of both the nonorthogonal mode (solid line) and the Gaussian input signal mode (dashed line). The nonorthogonal mode is narrower than the Gaussian mode because of the gain narrowing. It is interesting to note that this result holds throughout the amplifier, which may seem surprising because we would expect the narrower nonorthogonal mode to diffract faster than the Gaussian mode. The nonorthogonal mode stays narrower because gain guiding can compensate for the diffraction.

Figure 3 shows the index effect [8,9] when the input signal is detuned to the blue side of the Raman resonance. As before, the dashed line is the phase front of the Gaussian input signal mode and the solid line is the phase front of the

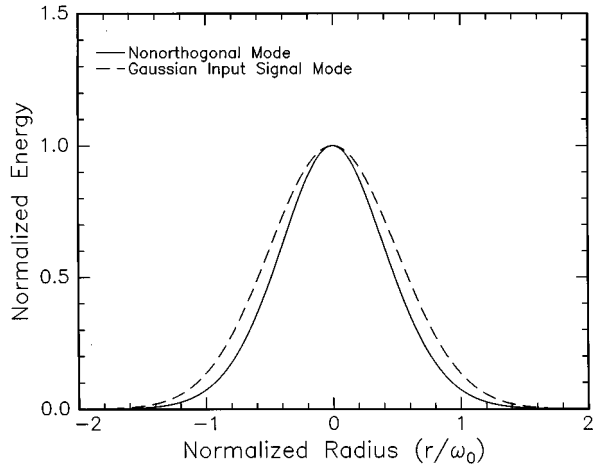

FIG. 2. Plot of the spatial structure of the dominant lowest-order nonorthogonal mode (solid line) and the Gaussian input signal mode. The nonorthogonal mode is narrower throughout the Raman amplifier due to gain guiding.

nonorthogonal mode when the detuning is set equal to zero, which turns off the index effect. The dot-dashed line is the phase front of the nonorthogonal mode when the input signal is detuned to the blue side of the Raman resonance. When the input signal is detuned to the blue side of the Raman resonance, the index guiding effect changes the wave front much like a focusing lens. The phase fronts are swept back less on the blue side of the Raman resonance than when $\Delta = 0$, indicating that focusing is occurring. The fact that the index effect is trying to guide the Stokes beam gives rise to the term index guiding.

Figure 4 shows the index effect when the input signal is tuned to the red side of the Raman resonance. The dashed and solid lines are the same as in Fig. 3. The dot-dot-dashed

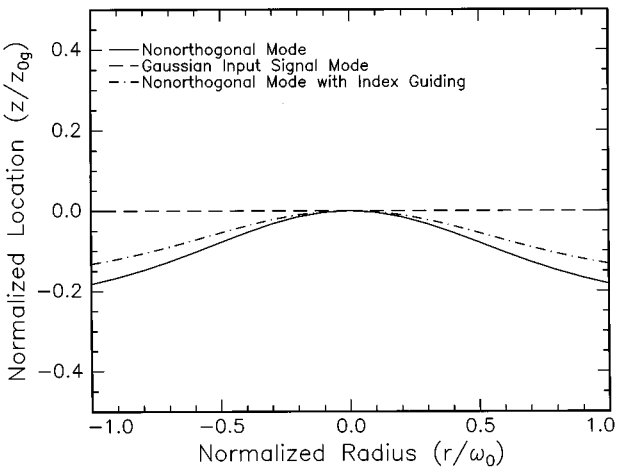

FIG. 3. Plot of the phase front of the dominant nonorthogonal mode including index guiding. The nonorthogonal mode for the on-resonance case is shown as a solid line, while the Gaussian input signal mode is shown as a dashed line. The nonorthogonal mode including the effect of index guiding is shown as a dot-dashed line. The index effect when the input signal is tuned to the blue side of the Raman resonance acts as a lens that tries to focus the nonorthogonal mode and leads to less curvature in this case.

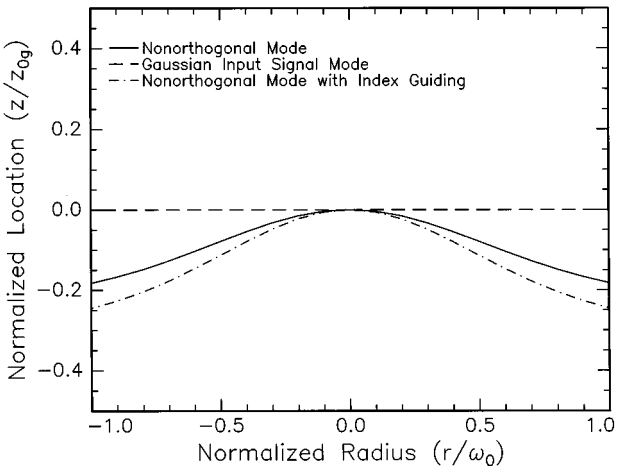

FIG. 4. Same as Fig. 3 except with the input signal tuned to the red side of the Raman resonance. The index effect acts as a defocusing lens in this case.

line is the contribution to the phase front due to the index effect. The phase front on the red side of the Raman resonance is swept back more than when $\Delta = 0$, indicating that defocusing is occurring.

The spatial structure of the nonorthogonal mode at $z/z_{0g} = 0$ is shown in Fig. 5. The dashed and solid lines are the same as in Fig. 2 and are shown again for reference. The dot-dashed line shows the intensity profile when the input signal is detuned to the blue side of the Raman resonance. The dotted line is the intensity profile line when the input signal is detuned to the red side of the Raman resonance. When the input signal is detuned to the blue (red) side of the Raman resonance the intensity profile is narrower (wider) than when the input signal is tuned to the Raman resonance

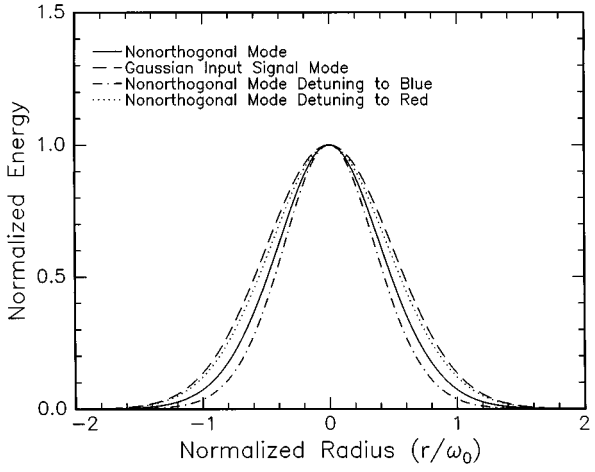

FIG. 5. Plot of the spatial structure of the dominant nonorthogonal mode. The solid and dashed lines are the same as in Fig. 2 and are shown again for reference. The dot-dashed line shows the spatial structure of the nonorthogonal mode when the input is tuned to the blue side of the Raman resonance and the dotted line shows the spatial structure when the input signal is tuned to the red side of the Raman resonance. Tuning to the blue (red) side of the Raman resonance causes the nonorthogonal mode to become narrower (wider) than when the input signal is tuned on resonance.

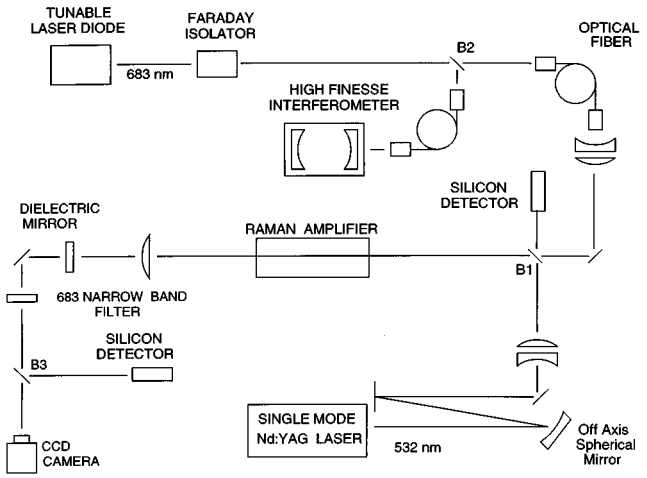

FIG. 6. Schematic of the experimental setup that is used to measure the radius of the amplified Stokes beam at 683 nm as a function of the detuning from the Raman resonance of the input signal Stokes beam.

and these result are consistent with the phase-front picture. The use of index guiding to enhance the output of the Raman amplifier is discussed in the next section. Before we proceed to a discussion about enhanced coupling in Sec. VI, an experiment is presented that allows the study of the spatial structure of the amplified Stokes beam at the output of the Raman amplifier.

IV. EXPERIMENT

The experimental setup that allows the study of gain guiding and index guiding as a function of the detuning Δ is shown in Fig. 6. The pump beam is provided by the frequency-doubled output at 532 nm of an injection seeded Nd:YAG laser (where YAG denotes yttrium aluminum garnet). The Nd:YAG laser has a temporal half-width at half maximum of 3.5 ns. The output of the Nd:YAG laser is reflected from an off axis spherical mirror to correct a slight astigmatism present in the output of the Nd:YAG laser [22]. The beam is then spatially filtered by a series of two pinholes (not shown in Fig. 6). The beam next passes through a series of lenses that focus the pump beam at the center of the Raman amplifier. After the lenses, the pump beam impinges on the dielectric mirror labeled $B1$ in Fig. 6. Part of the pump beam passes through $B1$ and is incident on a silicon energy detector that allows the monitoring of the pump energy for each shot of the pump laser. The rest of the pump beam is directed into the Raman amplifier.

The input signal or Stokes seed is provided by a continuous-wave tunable laser diode (TLD) with a center frequency of 683 nm. The output of the TLD is sent through a Faraday isolator, which prevents feedback from affecting the performance of the TLD. The input signal is then incident on beam splitter $B2$. Part of the input signal is sent via a single-mode optical fiber into a high-finesse interferometer (HFI) [23,24]. The HFI has a free spectral range of 23 600 MHz and a measured finesse of greater than 30 000, which allows the HFI to monitor the input signal relative frequency with sub-MHz resolution. The remainder of the input signal after $B2$ is launched into an optical fiber, which provides a convenient way of spatially filtering the input signal. The input signal then passes through a series of lenses that focus the input signal in the center of the Raman amplifier.

The input Stokes signal beam is combined with the pump beam at $B1$. The beams then travel collinearly through the Raman amplifier, which consists of H_2 at a pressure of 65 atm. Both the pump and input signal focus at the center of the 141-cm-long Raman amplifier. The measured Rayleigh range of the input signal was 31.4 cm and the measured Rayleigh range of the pump beam was 27.4 cm.

After exiting the Raman amplifier, the pump and amplified signal beam pass through a lens with a focal length of 100 cm, which allows the amplified Stokes beam at the exit of the Raman amplifier to be imaged onto a camera with a measured magnification of 1.6. After the imaging lens, the pump beam is blocked using a dielectric mirror that reflected the 532-nm pump beam but allowed the 683-nm amplified signal to pass. A narrow-band interference filter centered at 683 nm was placed behind the dielectric mirror to block any of the 532-nm pump beam that might have leaked through the dielectric mirror. This method of separating the pump beam and amplifier Stokes beam was found to be superior to using a pelin broca prism, which was found to introduce a significant astigmatism into the amplified Stokes beam. After the narrow-band filter, the amplified Stokes beam is incident on beam splitter $B3$. Part of the amplified field is sent to a silicon energy detector, which allows the energy of the amplified field to be monitored. The remainder of the amplified Stokes field is incident on a Pulnix TM-745 charge coupled device (CCD) camera. The CCD camera allowed the monitoring of the radius of the amplified Stokes field with the aid of a commercially available beam profile program [25].

Data are taken as follows. The TLD was slowly scanned across the Raman resonance. The pump energy, relative input signal frequency, amplified Stokes energy, and amplified Stokes beam radius were monitored and recorded using a personal computer for each shot of the pump laser. The pump energy was set at 890 μJ, which corresponds to a gain of $G=6.65$, where $\alpha=2.95\times10^{-9}$ cm/W [20] was used. The Raman linewidth was measure at 2880 MHz and agreed with the published value for the Raman linewidth [18] at the pressure of 65 atm, which was used in this experiment.

V. EXPERIMENTAL RESULTS

Numerical calculations that solve Eq. (1) by expanding the Stokes field over the nonorthogonal modal basis were performed for two cases. The first case includes the imaginary part of the Raman susceptibility only. In this case only gain guiding is occurring. In the second case the total Raman susceptibility is included and both gain and index guiding are occurring. Figure 7 is a plot of the radius calculated for the amplified Stokes beam at the exit of the Raman amplifier as a function of the detuning Δ.

The dashed line is the result of solving the wave equation for case 1 in which only gain guiding is occurring. At $\Delta=0$ the radius of the amplified Stokes beam at the exit of the amplifier is a minimum. At $\Delta=0$, the gain $[g(z,r)\Gamma^2/(\Gamma^2+\Delta^2)]$ is a maximum and the gain guiding effect that acts to narrow the amplified Stokes beam is the strongest. As Δ is

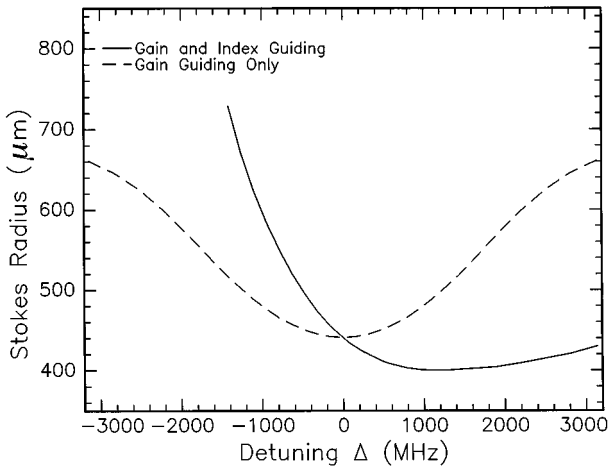

FIG. 7. Plot of the radius of the amplified Stokes beam as a function of detuning Δ. The dashed line represents the case where only gain guiding was included. The solid line is the case where both gain and index guiding are occurring. The radius for the solid line reaches a minimum at $\Delta=1400$ MHz, while the minimum radius for the dashed line is at $\Delta=0$ MHz.

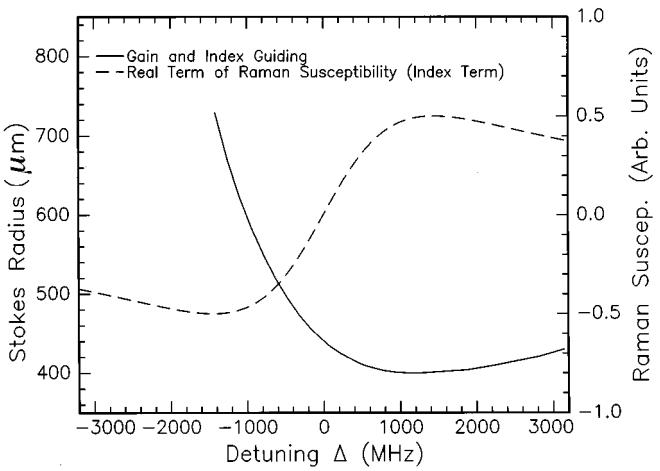

FIG. 8. The solid line is the same as in Fig. 7. The dashed line represents the real part of the Raman susceptibility. Notice that the minimum radius of the amplified Stokes beam occurs when the real term of the Raman susceptibility is at a maximum. For $\Delta>0$ ($\Delta<0$) the real part of the Raman susceptibility acts as a focusing (defocusing) lens.

detuned away from the Raman resonance so that $\Delta\neq 0$ the gain decreases and the gain guiding narrows the amplified Stokes beam less. At large detunings, the gain goes toward zero and the radius of the Stokes beam approaches the radius of the input signal.

The solid line in Fig. 7 is the result of solving the wave equation when the total Raman susceptibility is included in the wave equation. Both gain guiding and index guiding are occurring in this case. For $\Delta>0$ ($\Delta<0$) notice that the radius of the amplified Stokes beam is smaller (larger) than gain guiding predicts. This additional narrowing of the amplified Stokes beam results from index guiding. The index guiding is related to the real part of the Raman susceptibility and is proportional to $\Gamma\Delta/(\Gamma^2+\Delta^2)$. At $\Delta>0$ ($\Delta<0$), index guiding acts as a focusing (defocusing) lens, which focuses (defocuses) the amplified Stokes beam to a smaller (larger) spot size.

Figure 8 shows the correlation of the change in radius of the amplified Stokes as a function of detuning as the solid line with the change in the real part of the Raman susceptibility. The real term of the Raman susceptibility, which leads to index guiding, is shown in Fig. 8 as the dashed line. The strength of the index guiding is proportional to the magnitude of the real part of the Raman susceptibility. The minimum radius for the amplified Stokes beam occurs when the real part of the Raman susceptibility is at a maximum at $\Delta=1440$ MHz. When $\Delta>0$ the real part of the Raman susceptibility acts to focus the amplified Stokes. For $\Delta<0$ the real part of the Raman susceptibility acts to defocus the amplified Stokes. At $\Delta<-1200$ MHz, the Stokes radius has become large enough so that only a small percentage of the amplified Stokes beam overlaps the gain profile and hence the Stokes beam experiences a very weak gain.

Figure 9 is a plot of the normalized Stokes energy as a function of detuning Δ. The pluses represent experimental data taken by scanning the TLD across the Raman resonance. The dashed line is a least-squares Gaussian fit to the data and the solid line is the theoretical results from solving Eq. (1). The on-resonance case occurs when $\Delta=0$ MHz. Notice that the peak Stokes output is shifted to the blue side of the Raman resonance. The shift results from the focusing of the amplified Stokes beam due to index guiding [9]. The peak Stokes output occurs at $\Delta=230$ MHz. The peak in the Stokes output results from the competition between an increase in the gain due to a narrower Stokes beam, which is caused by index guiding (see Figs. 7 and 8) and a loss in gain [which is proportional to $\Gamma^2/(\Gamma^2+\Delta^2)$] due to the detuning Δ.

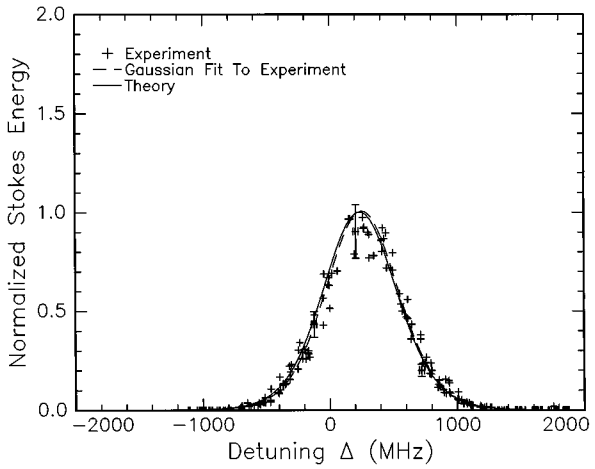

FIG. 9. Plot of the normalized Stokes output energy as a function of detuning from the Raman resonance. The +'s correspond to experimental data, the dashed line is a Gaussian least-squares fit to the data, and the solid line is the theoretical predictions from solving the wave equation with a nonorthogonal modal expansion for the Stokes field. The on-resonance case ($\Delta=0$) was determined by lowering the gain, which causes the peak Stokes output to move toward $\Delta=0$. Notice that the peak Stokes output is not at $\Delta=0$, but is shifted to the blue side of the Raman resonance by $\Delta=230$ MHz.

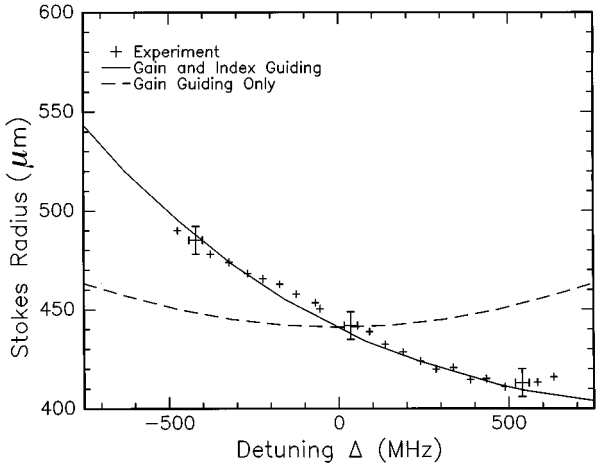

FIG. 10. Plot of the radius of the amplified Stokes beam at the exit of the Raman amplifier. The dashed and solid line are the same as Fig. 7. The +'s represent experimental measurements. The experimental measurements are in agreement with the predictions of the wave equation when the total Raman susceptibility is included, allowing for both gain and index guiding.

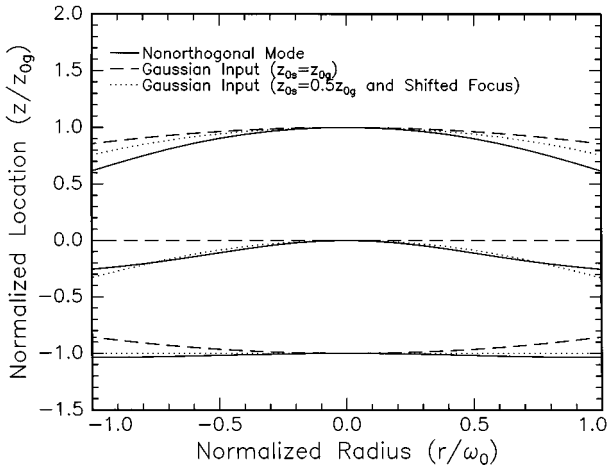

FIG. 11. Plot of the phase fronts of the nonorthogonal mode (solid line), Gaussian input signal mode (dashed line), and modified Gaussian input signal mode (dotted line). The nonorthogonal mode and modified Gaussian input match much better than the nonorthogonal mode and unmodified Gaussian input, indicating that the modified input enhances the performance of the Raman amplifier.

The Raman resonance at $\Delta=0$ was determined as follows [9]. The shift in the peak Stokes output is a function of the gain of the Raman amplifier. As the gain is lowered, the index effect has a smaller focusing effect on the amplified Stokes beam and hence the increase in the gain due to a narrower Stokes beam overlapping a more intense part of the pump beam becomes negligible. At low gains the peak of the Stokes output occurs near $\Delta=0$. Experimentally, the gain was lowered by lowering the pump energy and the TLD was swept across the Raman resonance to find $\Delta\approx 0$ MHz.

Figure 10 shows the radius of the amplified Stokes beam at the exit of the Raman amplifier as a function of the detuning. The solid and dashed lines are the same as in Fig. 7 and the pluses are the experimental points. The detuning range Δ was limited in the experiment to approximately ± 500 MHz, where the gain was large enough for the CCD camera to measure the amplified Stokes beam. Beyond this detuning range, the gain was too small so that the CCD camera could not measure the amplified Stokes beam. Each experimental point consists of an average of at least 25 pump shots within a frequency window of 40 MHz. The experimental measurements clearly indicate that both gain guiding and index guiding are needed to account for the change in the Stokes radius in the Raman amplifier as the detuning is varied.

VI. ENHANCED COUPLING

The most efficient coupling of the input signal into the lowest-order nonorthogonal mode supported by the Raman amplifier occurs when the projection of the Gaussian input signal mode onto the lowest-order nonorthogonal mode is maximized. This projection is maximized when the modes have identical phase fronts. The overlap of the phase fronts of the Gaussian input signal mode and lowest-order nonorthogonal mode is poor, as seen in Fig. 1, when the input seed and nonorthogonal mode focus at the same location with the same Rayleigh range. By changing the position of the focus and Rayleigh range of the input signal, we can force the phase fronts at the input to the Raman amplifier to better overlap the lowest-order nonorthogonal mode and hence enhance the input coupling of the Raman amplifier.

Figure 11 shows that by changing the location of focus and Rayleigh range of the input signal Gaussian mode, its phase fronts can better overlap the nonorthogonal mode. The solid lines are the nonorthogonal mode phase fronts whose shape are determined by the Rayleigh range and power of the pump laser. We consider these phase fronts to be fixed and show that varying the characteristics of the input signal Gaussian mode can enhance coupling into the amplifier. The dashed lines are the phase front of the input signal Gaussian mode with a Rayleigh range and location of focus the same as the pump. The dotted lines are the phase fronts for an input signal Gaussian mode with a Rayleigh range one-half that of the pump and the focus shifted toward the entrance of the Raman amplifier. Notice that the dotted line and solid line match much better than the dashed line and solid line. This indicates that the input signal Gaussian mode with a shorter Rayleigh range and shifted focus relative to the pump will better overlap the lowest-order nonorthogonal mode and thus improve the performance of the Raman amplifier.

Figure 12 is a more detailed study of how the shift in location of the focus can affect the output of the Raman amplifier. The dashed line shows the output Stokes energy as a function of the focal position of the input signal when the pump and input signal have the same Rayleigh range. The output Stokes energy in this plot has been normalized so that when the pump and input signal focus at the same location with the same Rayleigh range the output Stokes energy is unity. When $z_{0s}=z_{0g}$ the output of the Raman amplifier is enhanced by 5% by shifting the focus of the input signal toward the entrance of the Raman amplifier by approximately one-half a Rayleigh range. The solid line is the output Stokes energy as a function of the relative focus when the Rayleigh range of the input signal is one-half that of the

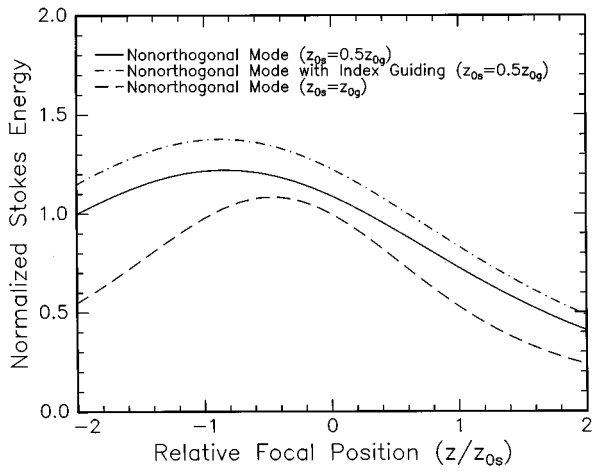

FIG. 12. Plot of the normalized output Stokes energy as a function of the relative focal position of the Gaussian input signal and pump focus. When $z_{0s}/z_{0g}=1$, shifting the focus of the input signal by approximately one-half a Rayleigh range yields a 5% increase of the output Stokes energy. For $z_{0s}/z_{0g}=0.5$, shifting the focus of the input signal by approximately one Rayleigh range increases the Stokes output by as much as 20%. When the input signal is detuned to the blue side of the Raman resonance the Stokes output is increased by a maximum of approximately 40%.

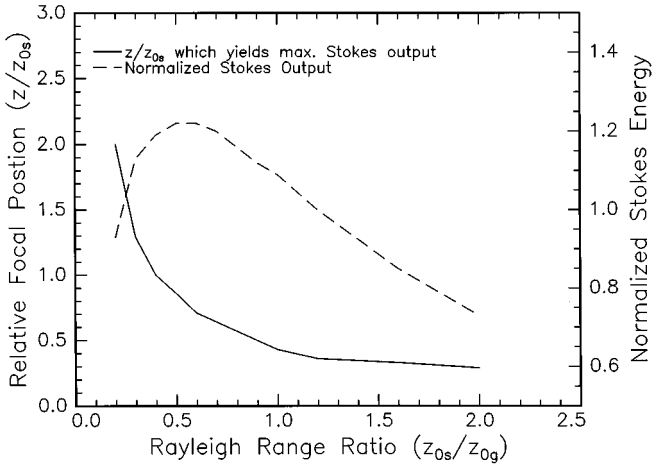

FIG. 13. Plot of the shift in focus that yields the maximum Stokes output as a function of the Rayleigh range of the input signal. Also shown is the increase in Stokes output at z_{0s}/z_{0g} when the input signal is modified to yield the maximum output Stokes energy. The maximum Stokes output occurs when the Rayleigh range ratio is $z_{0s}/z_{0g}=0.5$ and the relative focal position is shifted by $z/z_{0s}=0.86$.

pump. When the focus of the seed beam is shifted toward the entrance of the Raman amplifier by approximately one Rayleigh range the Stokes output is enhanced by over 20%. The output Stokes energy is further increased when the input signal is detuned to the blue side of the Raman resonance. The dot-dashed line in Fig. 12 is the Stokes output for $z_{0s}=0.5z_{0g}$ and detuning to the blue side of the Raman resonance. The output is enhanced by over 40% when the input signal has been modified and tuned to the blue side of the Raman resonance. This implies that by carefully setting up an optical amplifier the output can be significantly increased without changing the pump or input signal power.

The enhanced performance of the Raman amplifier due to index guiding is explained as follows. When the input signal is tuned to the blue side of the Raman resonance, the real part of the Raman susceptibility acts like a focusing lens, as seen in Figs. 3 and 5. Because the Stokes beam is focused to a smaller spot, it overlaps a more intense part of the pump beam and hence experiences a larger gain.

The effect of different Rayleigh ranges and different shifted locations of focus on the Stokes output are studied in Fig. 13. The shift of the focus that yields the maximum Stokes output for a particular z_{0s}/z_{0g} ratio is plotted as the solid line in Fig. 13. A larger shift in focus for a smaller Rayleigh range ratio of z_{0s}/z_{0g} is needed to maximize the Stokes output. The dashed line is the normalized Stokes output for a particular z_{0s}/z_{0g} when the focus of the input signal has been shifted to yield the maximum Stokes output from the Raman amplifier. The Stokes output has been normalized so that when $z_{0s}/z_{0g}=1$ and the input signal and pump focus at the same location the Stokes output is unity. At $z_{0s}/z_{0g}=0.7$ the Stokes output has been enhanced by over 20%. Including index guiding will further enhance the gain as seen in Fig. 12.

VII. CONCLUSION

Nonorthogonal modes conveniently describe the Stokes field in a Raman amplifier. The nonorthogonal modes result from a competition between gain guiding and diffraction. In the high gain limit only the lowest-order nonorthogonal mode is needed to describe the growth of the Stokes field and for this reason the nonorthogonal mode is a natural choice for describing the output from a Raman amplifier.

An experiment was presented in which the radius of the amplified Stokes beam was measured as a function of detuning of the input signal. The experimental results showed that the radius of the amplified Stokes beam decreases as the input seed is tuned to the blue side of the Raman resonance. This result does not agree with the predictions of theories that include only the imaginary part of the Raman susceptibility and allow only for gain guiding. When the total Raman susceptibility is included, which allows both gain and index guiding in the theory, the theory accurately predicts the experimental results.

Gain guiding effects result in a narrower beam with phase fronts that are swept back from the input signal Gaussian mode. The swept back phase fronts of the nonorthogonal mode indicate a narrower beam that tends to diffract faster than the free space mode. The phase fronts and spatial structure of the lowest-order nonorthogonal mode is further complicated by index effects that tend to either focus or defocus the Stokes beam depending on which side of the Raman resonance the input signal is tuned to. When the input signal is tuned to the blue side of the Raman resonance the phase fronts of the nonorthogonal mode are swept back less than when the input signal is tuned to the Raman resonance. This index guiding effect leads to an enhanced output from the Raman amplifier.

The question of coupling a Gaussian input signal to the lowest-order nonorthogonal mode requires that the phase fronts of the input signal match the phase fronts of the

lowest-order nonorthogonal mode as closely as possible at the input to the Raman amplifier. The nonorthogonal mode phase fronts are complicated and caused by the interplay of the nonlinear effects of gain and index guiding with diffraction. By judiciously choosing the proper shifting of the focus and Rayleigh range of the input signal relative to the pump and by detuning the input signal to the blue side of the Raman resonance the input coupling and performance of the Raman amplifier can be enhanced.

ACKNOWLEDGMENT

This work was supported by National Science Foundation Grant No. PHY-9424637.

[1] H. A. Haus and S. Kawakami, IEEE J. Quantum Electron. **21**, 63 (1985).
[2] A. E. Siegman, Phys. Rev. A **39**, 1253 (1989).
[3] J. G. Wessel, P. R. Battle, and J. L. Carlsten, Phys. Rev. A **50**, 2587 (1994).
[4] J. G. Wessel, K. S. Repasky, and J. L. Carlsten, Phys. Rev. A **54**, 2408 (1996).
[5] K. Peterman, IEEE J. Quantum Electron. **QE-15**, 566 (1979).
[6] S. J. Kuo, D. T. Smithey, and M. G. Raymer, Phys. Rev. Lett. **20**, 2605 (1991).
[7] P. R. Battle, J. G. Wessel, and J. L. Carlsten, Phys. Rev. A **48**, 707 (1993).
[8] J. Mostowski and B. Sobolewska, Phys. Rev. A **34**, 3109 (1986).
[9] K. S. Repasky and J. L. Carlsten, Phys. Rev. A **54**, 4528 (1996).
[10] B. N. Perry, P. Rabinowitz, and D. S. Bomse, Opt. Lett. **10**, 146 (1985).
[11] S. Logl, M. Scherm, and M. Maier, Phys. Rev. A **52**, 657 (1995).
[12] J. G. Wessel, R. S. Repasky, and J. L. Carlsten, Phys. Rev. A **53**, 1854 (1996).
[13] A. Yariv, *Quantum Electronics*, 3rd ed. (Wiley, New York, 1989).
[14] P. Amendt, R. A. London, and M. Strauss, Phys. Rev. A **44**, 7478 (1991).
[15] M. Segev, B. Crosignami, and A. Yariv, Phys. Rev. Lett. **68**, 923 (1992).
[16] G. Duree, G. Salamo, M. Sergev, A. Yariv, B. Crosignami, P. DiPorto, and E. Sharp, Opt. Lett. **19**, 1195 (1994).
[17] B. N. Perry, P. Rabinowitz, and M. Newstein, Phys. Rev. A **27**, 1989 (1983).
[18] W. K. Bischel and M. J. Dyer, Phys. Rev. A **33**, 3113 (1986).
[19] The gain coefficient G_p can be related to physical parameters that are typical in a Raman amplifier experiment as $G_p = \alpha P_p / \lambda_g$, where α is the plane-wave gain coefficient, P_p is the peak pump power, and λ_g is the pump wavelength.
[20] W. K. Bischel and M. J. Dyer, J. Opt. Soc. Am. B **3**, 677 (1986).
[21] I. H. Deutsch, J. C. Garrison, and E. M. Wright, J. Opt. Soc. Am. B **8**, 1244 (1991).
[22] A. Bruschi, S. Cirant, G. Granucci, A. Simonetto, and G. Solari, Int. J. Infrared Millim. Waves **15**, 1413 (1994).
[23] K. S. Repasky, L. E. Watson, and J. L. Carlsten, Appl. Opt. **34**, 2615 (1995).
[24] K. S. Repasky, J. G. Wessel, and J. L. Calrsten, Appl. Opt. **35**, 609 (1996).
[25] Big Sky Laser Technologies, Bozeman, MT.